

Physical Properties of Mercaptopyruvic-acid Layer Formed on Gold Surfaces

Jin-Won Park

*Department of Chemical Engineering, College of Engineering, Seoul National University of Science and Technology, Seoul 139-743, Korea. *E-mail: jwpark@seoultech.ac.kr*

Received June 7, 2011, Accepted June 24, 2011

We studied the physical properties of the mercaptopyruvic-acid layer formed on gold surfaces, which has the interactions with the titanium dioxide surface for design of gold- titanium dioxide distribution. Surface force measurements were performed, using the atomic force microscope (AFM), between the surfaces as a function of the salt concentration and pH value. The forces were analyzed with the DLVO (Derjaguin-Landau-Verwey-Overbeek) theory, to evaluate the potential and charge density of the surfaces quantitatively for each salt concentration and each pH value. The difference in the properties reflected the effect of the isoelectric point on the surface forces. The forces were interpreted for the evaluation with the law of mass action and the ionizable groups on the surface. The salt concentration dependence of the surface properties, found from the measurement at pH 8.0, was consistent with the prediction from the law. It was found that the mercaptopyruvic-acid layer had higher values for the surface charge densities and potentials than the titanium dioxide surfaces at pH 8, which may be attributed to the ionized-functional-groups of the mercaptopyruvic-acid layer.

Key Words : Mercaptopyruvic-acid, Gold surface, TiO₂ surface, AFM, DLVO theory

Introduction

A lot of attention have been paid to materials composed of gold and a semiconducting support for numerous applications such as surface patterning, catalysis, photocatalysis, and photovoltaic cells.¹⁻⁶ For the catalysis, the oxidation on the materials by light generates electron-transfer processes that may be used for the degradation of the organic pollutants.⁷ Activity and selectivity of such materials and catalysts is determined by the distribution.⁸

Different methods were devised in the last decade for the preparation of Au-TiO₂ catalyst materials such as metal ion impregnation and deposition-precipitation followed by drying, calcinations, and reduction.⁹ During these procedures, the Au particles or clusters are formed directly on the support. However, it is found that there are some drawbacks in these approaches. The non-uniform distribution of the precursors in the solution, caused by the gravitational forces, leads to various dispersions of the resulting metal particles. Additionally, the essential thermal treatment generates severe agglomeration of the materials and may cause undesirable change in the support chemistry through ionic diffusion.⁵ These problems lower the activity and selectivity of the materials. Therefore, alternative approach for catalyst preparation has been suggested. The approach is based on the preparation of metallic Au⁰ particles in solution, followed by deposition of the particles on the TiO₂.^{5,10} The particles were passivated with ligands such as phosphines and thiols, which play a role to prevent the particles from agglomeration in solution.¹¹⁻¹³ After the deposition, the ligands can be removed by calcinations of the material and thiolate oxidation and rinse with solvents.¹⁴⁻¹⁷

The atomic force microscope (AFM) was proved as a

useful technique to monitor the behavior of gold particles.¹⁸ Among surface characterization techniques, the AFM is capable of providing insight for analysis of surface properties of a colloidal particle and a flat surface as a function of separation.¹⁹ The properties, especially electrostatic properties, were estimated by comparing the normalized surface forces, acquired from the AFM, with the theoretical surface forces that are Derjaguin-Landau-Verwey-Overbeek (DLVO) theory forces.²⁰ The properties are used as an indicator for electrostatic repulsion between particles, which may be strongly relevant to the particle distribution that the activity and selectivity of the catalyst depends on. In this research, we investigated the effects of the mercaptopyruvic-acid layer formation on gold surfaces that have the interactions with the titanium dioxide surface.

Experiments

Surface Preparation. The gold surfaces were prepared by using a high-vacuum electron beam evaporator to sequentially deposit a 5 nm chrome adhesion layer and a 100 nm gold layer on the silicon wafers. Immediately prior to use, the gold surfaces were immersed in a 3:1 solution of 96% sulfuric acid and 30% hydrogen peroxide at 60-80 °C for 10 min. The gold surface was exposed to a solution of 10 mM mercaptopyruvic-acid, 100 mM potassium nitride, at pH 4 for several hours at room temperature, followed by rinsing with a running buffer. The mercaptopyruvic-acid layer formation on the gold surface was confirmed using qualitative surface force measurement in 100 mM potassium nitride at pH 4. In order to perform quantitative surface force measurements, the solution was replaced with a running buffer (six running buffers used in this research – 1, 10, and

100 mM potassium nitride at pH 4 and 8, respectively) by injecting the buffer into the fluid cell by a syringe equipped with a needle. The titanium dioxide surfaces were made on the silicon wafer by sputtering titanium in an argon-oxygen environment for 40 min. For the sputtering, an RF magnetron source was operated at 2 kW. Prior to sputtering, any native oxide layer of the wafers was removed by immersion in hydrofluoric acid. The total pressure was 5×10^{-6} bar, with argon and oxygen flow rates of 6 and 1.2 dm³/min, respectively. During the sputtering, the substrates were rotated continuously around the target. The substance to target distance was 7 cm, and target diameter was 20 cm. The characteristics of the TiO₂ layers were identical with those of the gold surfaces.

AFM Measurements. Topology images and surface force measurements were made with a 3-D Molecular Force Probe AFM (Asylum Research, Santa Barbara, CA) with a closed-loop piezo-electric transducer. Commercially available cantilevers (Olympus, Shinjuku-ku, Tokyo, Japan), microfabricated with silicon nitride, with 15–25 nm curvature tip were used for topographic imaging and qualitative surface force measurements. Quantitative surface force measurements were carried out with titanium dioxide spheres (Microspheres-Nanospheres, Cold Spring, NY) of 3 μm diameter that were attached to the microfabricated cantilevers, shown in Figure 1. The sphere was immobilized at the end of the cantilever with UV-sensitive adhesive (Norland Products, New Brunswick, NJ). Exposure of the adhesive to the UV light source and surface cleaning were achieved simultaneously in an ozone cleaning apparatus (Jelight, Irvine, CA). It was observed that the attachment of the sphere and the ozone clean did not cause any change in the response of the cantilever. The spring constant of the cantilever was found using the thermal frequency spectrum of the cantilever.²¹

Theory

The forces between interacting electrostatic double layers have been explained with the theory of Derjaguin-Landau-Verwey-Overbeek (DLVO).²² The theory describes that the total interaction energy between two plates is the sum of an attractive van der Waals component (V_A), an electrostatic

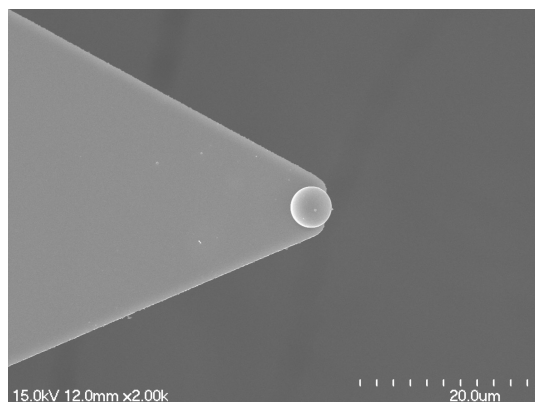


Figure 1. Titanium dioxide sphere-attached-cantilever.

repulsion or attraction (V_E), and an additional repulsion (V_S) at close separations resulting from the presence of ordered solvent layers.^{23–26}

According to the Derjaguin approximation, the force between a sphere of radius R_T and a plate can be expressed to the energy between plates by the relation²⁷

$$F/R_T = 2\pi(V_A + V_E + V_S) \quad (1)$$

The van der Waals energy (V_A) in the non-retarded situation is related by an equation of the form

$$V_A = -A_H/12\pi d^2 \quad (2)$$

where A_H is the Hamaker constant and d is the separation distance.²⁸ The Hamaker constant of the mercaptopyruvic-acid layer is reasonably approximated into 7.0×10^{-20} J, since the most component of the layer is hydrocarbon.²⁹ The Hamaker constant of the TiO₂ surface is 5.0×10^{-20} J.³⁰ The electrostatic interaction (V_E) can be calculated by integrating the electrostatic force.^{31–33} Therefore, the interaction for a 1:1 Electrolyte is

$$V_E = -\int_{\infty}^D \left\{ 2n^0 kT \left[\cosh\left(\frac{ze\psi}{kT}\right) - 1 \right] - \frac{\epsilon}{2} \left(\frac{d\psi}{dz}\right)^2 \right\} dz \quad (3)$$

where ψ is the electrostatic potential. The first term in eq. (3) is a repulsive osmotic component that results from the accumulation of charge in the gap between the plates, and the second is a Maxwellian stress that represents an induced charge and is always attractive. To find out the value of V_E explicitly, the electrostatic potential should be known as a function of distance between the surfaces. The potential can be obtained from the solution of the Poisson-Boltzmann equation

$$\frac{d^2\psi}{dz^2} = -\frac{1}{\epsilon_0\epsilon_r} \sum_i n_i^0 z_i e \exp\left(-\frac{z_i e \psi}{kT}\right) \quad (4)$$

In general, the complete nonlinear form of eq. (4) must be solved, which can be found only by numerical techniques.³⁴ Based on the solution of eq. (4), eq. (3) was integrated with a Simpson's 3/8 rule. The additional repulsive force (V_S) in eq 1 is considered to arise from the presence of ordered solvent layers and can be described by a decaying oscillatory force.³⁵ This repulsive force is not clearly understood and will be neglected in the calculations presented here.

Results and Discussion

The surface forces were measured to characterize the structures of the mercaptopyruvic-acid layer formed on the gold surfaces, using the AFM. Constant force AFM images were acquired on the gold surfaces, mercaptopyruvic-acid-formed-gold surfaces, and TiO₂ surfaces. The morphologies of these surfaces were dominated by the polycrystalline structures of the evaporated metals with 1.5 nm roughness, which were essentially indistinguishable on the surfaces (results were not shown). Phase separation has been observed with AFM in lipid films and is easily visualized as micro-

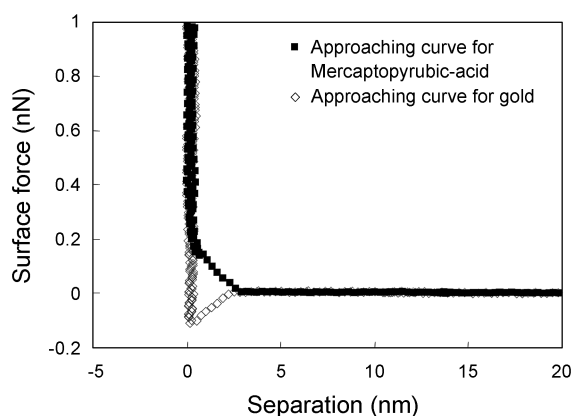


Figure 2. Force-distance curve between a silicon nitride probe and the mercaptopyruvic-acid layer formed in 100 mM potassium nitride at pH 4.

meter-sized domains in the contact imaging mode.³⁶ No observation of these domains on the surfaces strongly suggests that the mercaptopyruvic-acid forms homogeneous layer on the gold surfaces.

For the confirmation of the formation of mercaptopyruvic-acid layer on the gold surfaces, AFM forces were measured on the gold surfaces and the mercaptopyruvic-acid-formed-gold surfaces with 20-nm-radius probes. As shown in Figure 2, only repulsions were observed in approaching force-distance curves for measurements between a silicon nitride probe and the mercaptopyruvic-acid layer formed in 100 mM potassium nitride at pH 4. The repulsions were approximately 0.2 nN in the distance of less than 2.0 nm from the layer, while the force curve of the gold surface showed a negative force that means an attractive region. The repulsion, not found on the gold surfaces, appears to be generated by the lower Hamaker constant and more hydration of the mercaptopyruvic-acid layer.²⁹ The clear difference of the force curve indicates that the mercaptopyruvic-acid layers were well-formed on the gold surfaces.

The titanium dioxide surface should be theoretically analyzed earlier prior to the analysis of the force curves between the titanium dioxide surface and the mercaptopyruvic-acid layer surface, because the analysis is based on the asymmetric boundary conditions. Therefore, as a first, the surface charge density and potential of the 3- μm -diameter titanium dioxide sphere were estimated from the analysis of the force curves between the sphere and the titanium dioxide surface. The approaching force curves presented in Figure 3 were acquired as a function of the separation between the titanium dioxide sphere and the titanium dioxide surface in three running buffers at pH 8. The surface forces were completely repulsive in the long-range that was mainly determined by the ionic strength of the solution. The exponential dependence of the repulsive force on distance was consistent with double-layer forces between surfaces of like charge in aqueous solutions. At a distance of less than 2.0 nm from the layer, short-range repulsive forces were clearly found that may be attributed to the steric forces and the inherent roughness of the

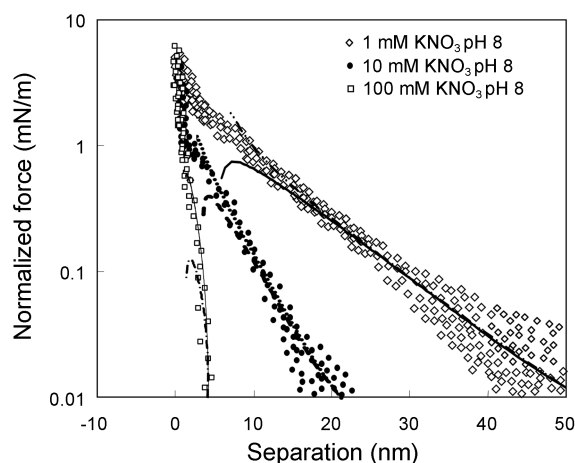


Figure 3. Approaching force curve as a function of the separation between the sphere and the surface of the titanium dioxide in 1, 10, 100 mM potassium nitride at pH 8.

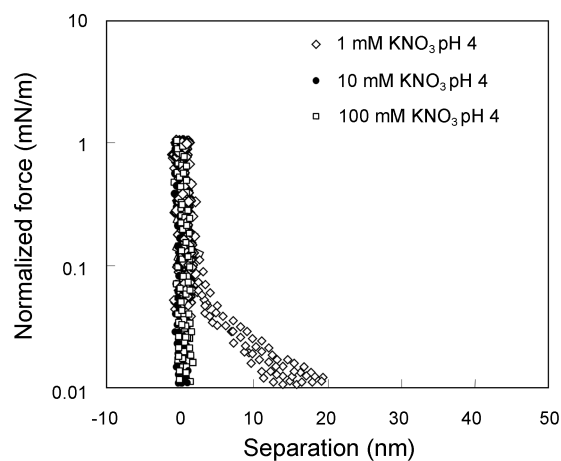


Figure 4. Approaching force curve as a function of the separation between the sphere and the surface of the titanium dioxide in 1, 10, 100 mM potassium nitride at pH 4.

surfaces.^{37,38}

In terms of the long-range, the surface forces were less repulsive at pH 4 than pH 8 for potassium nitrate solutions. The forces were presented in Figure 4 for pH 4. The forces, measured in 1 mM potassium nitrate solution at pH 4, were less repulsive than those at pH 8 due to the iso-electric point of TiO_2 . At pH 4, the forces were not even found in 10 mM and 100 mM potassium nitrate solution. That is, at pH 4, the electrostatic forces appeared not to be the dominant component in the long range of the surface forces on the TiO_2 surface in 10 mM and 100 mM potassium nitrate solution. Therefore, the force curves acquired for 10 mM and 100 mM potassium nitrate solution at pH 4 were not appropriate to be analyzed with the DLVO theory.

From the analysis, the titanium dioxide surface was characterized for the constant surface potential or charge density of the surfaces. The surface potential of the titanium dioxide surface is found -10 to -100 mV at pH 8.0. The results of this theoretical analysis are summarized in Table 1. Our results seem to be consistent with the findings previ-

Table 1. Electrostatic properties of the titanium dioxide surfaces

pH 8			
	1 mM Potassium nitrate	10 mM Potassium nitrate	100 mM Potassium nitrate
Surface potential (mV)	-42 ± 4	-27 ± 3	-18 ± 3
Surface charge density (10 ⁻³ C/m ²)	-3.0 ± 0.3	-6.3 ± 0.7	-12.0 ± 1.5
pH 4			
	1 mM Potassium nitrate	10 mM Potassium nitrate	100 mM Potassium nitrate
Surface potential (mV)	9 ± 1	- ^a	- ^a
Surface charge density (10 ⁻³ C/m ²)	0.6 ± 0.2	- ^a	- ^a

^aElectrostatic property was not acquired.

ously published by those of Feiler *et al.*, where AFM was utilized for the characterization of the titanium dioxide surface in a 1 mM potassium nitrate solution and the surface potential was -43 mV at pH 8.³⁰ The change from negative to positive potential is caused by the change from negative to positive values at an isoelectric point of pH 4.3.³⁰ Since the analysis could not be performed for the surface forces of the 10 mM and 100 mM potassium nitrate solution at pH 4, there were no results for the surface potential and charge density of the TiO₂ for them.

As presented in Table 1, the surface potential of the titanium dioxide surface increased monotonically with decreasing ionic strength, while the surface charge density decreased monotonically with decreasing ionic strength at pH 8. The salt concentration dependence of the surface has been described using the model developed with ionizable groups based on the law of mass action.³⁹ The relation between surface charge density (σ), surface potential (ψ_o), and salt concentration may be determined by the simultaneous solution of the law of mass action

$$\sigma = \sigma_o \frac{1}{1 + K_a [H^+] \exp\left(-\frac{e\psi_o}{kT}\right) + K_b [K^+] \exp\left(-\frac{e\psi_o}{kT}\right)} \quad (5)$$

and Graham's equation

$$\sigma = \sqrt{8\epsilon\epsilon_o kT} \sinh\left(\frac{e\psi_o}{kT}\right) \sqrt{([K^+] + [H^+])} \quad (6)$$

where σ_o is the maximum surface charge density, ϵ is the dielectric constant of water, ϵ_o is the permittivity of free space, e is the electronic charge constant, k is the Boltzmann's constant, T is temperature. The salt concentration dependence of the surface properties, found from the measurement at pH 8.0, was consistent with the prediction from the model.

After the characterization of the titanium dioxide sphere surface, the force measurements were performed on the mercaptopyruvic-acid layer formed on the gold surfaces with the titanium dioxide sphere. The surface potential and charge density of the mercaptopyruvic-acid layer surfaces were found by analyzing the force curves. Figure 5 shows the results of force measurements made on the mercap-

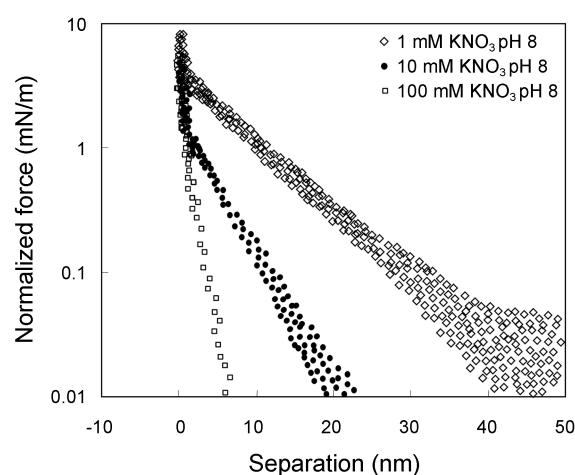


Figure 5. Approaching force curve as a function of the separation between the titanium dioxide sphere and the mercaptopyruvic-acid layer in 1, 10, 100 mM potassium nitrate at pH 8.

pyruvic-acid layers in the three running buffers at pH 8. The long-range surface forces were purely repulsive and varied in range with ionic strength in a manner that was consistent with double-layer forces. The forces were quantitatively analyzed with the DLVO theory at asymmetric boundary conditions. In Table 2, the surface potentials and charge densities on the mercaptopyruvic-acid layer surfaces were summarized as a function of ionic strength and pH value.

The surface potential and charge density of the mercaptopyruvic-acid layer surface were also described, as a function of the salt concentration, with the model. It was found that the mercaptopyruvic-acid layer had higher values for the surface charge densities and potentials than the titanium dioxide surfaces at pH 8, which may be attributed to the ionized-functional-groups of the mercaptopyruvic-acid layer. In 1 mM potassium nitrate solution at pH 4, the long-range forces were purely attractive on the mercaptopyruvic-acid layer surface (data are not presented), while they were repulsive on the titanium dioxide surfaces. This result was predictable due to pK_a of the mercaptopyruvic-acid and the iso-electric-point of TiO₂. The long-range forces were also not found on the mercaptopyruvic-acid layer surface in 10 mM and 100 mM potassium nitrate solutions at pH 4,

Table 2. Electrostatic properties of the mercaptopyrivic-acid layer

	pH 8		
	1 mM Potassium nitrate	10 mM Potassium nitrate	100 mM Potassium nitrate
Surface potential (mV)	-86 ± 5	-53 ± 5	-32 ± 3
Surface charge density (10 ⁻³ C/m ²)	-14 ± 2	-25 ± 3	-48 ± 5
	pH 4		
	1 mM Potassium nitrate	10 mM Potassium nitrate	100 mM Potassium nitrate
Surface potential (mV)	-21 ± 2	- ^a	- ^a
Surface charge density (10 ⁻³ C/m ²)	-1.8 ± 0.2	- ^a	- ^a

^aElectrostatic property was not acquired.

because they were not on the titanium dioxide surfaces in the solutions.

From the observations described above, it is obvious that the electrostatic forces between the mercaptopyrivic-acid layer surface and the TiO₂ surface were adjustable quantitatively with a salt concentration and pH value. It was believed that the kinetics of the adsorption for either TiO₂ particles to mercaptopyrivic-acid layer-coated-gold surface or mercaptopyrivic-acid layer-coated-gold particles to TiO₂ surface might be also adjustable, because the adsorption is determined by the forces between the surfaces. In addition, the kinetics is related to the distribution of the particles adsorbed to the surface. For the design of the distribution of the particles adsorbed to the surfaces, the surface forces as a function of the salt concentration and the pH value seem to be important. Performance of catalysts may be mainly affected by the distribution, eventually the salt concentration and the pH value.

In conclusion, the surface forces between the mercaptopyrivic-acid layer-coated-gold surface and the TiO₂ surface were measured as a function of the salt concentration and pH value using the AFM. From the force analysis with the DLVO theory, the surface potential and charge density of the surfaces were quantitatively estimated for each of salt concentration and pH value. The relation between the salt concentration, and surface potential and charge density was described with the law of mass action, and the pH dependence was with the ionizable groups on the surface. The electrostatic properties between the mercaptopyrivic-acid layer-coated-gold surface and the TiO₂ surface have not been quantitatively made so far, although the properties are the fundamental information to adjust the distribution of the TiO₂ domain on the gold surface or vice versa. In this study, it is obvious that the formation of the mercaptopyrivic-acid layer on gold surfaces may be useful to design the novel structure of either gold particle adsorbed to the TiO₂ surface or vice versa by understanding the electrostatic interactions.

Acknowledgments. We thank all of members of Department of Chemical Engineering, the Seoul National University of Science and Technology for help and valuable discussions.

References

- Murdoch, M.; Waterhouse, G. I. N.; Nadeem, M. A.; Metson, J. B.; Keane, M. A.; Howe, R. F.; Llorca, J.; Idriss, H. *Nature Chemistry* **2011**, *3*, 489.
- Peter, A.; Baia, M.; Toderas, F.; Lazar, M.; Tudoran, L. B.; Danciu, V. *Studia Universitatis Babeş-bolyai Chemia* **2009**, *54*, 161.
- Kowalska, E.; Mahaney, O. O. P.; Abe, R.; Ohtani, B. *J. Catalys.* **2010**, *12*, 2344.
- Perlich, J.; Memesa, M.; Diethert, A.; Metwalli, E.; Wang, W.; Roth, S. V.; Timmann, A.; Gutmann, J. S.; Muller-Buschbaum, P. *Chem. Phys. Chem.* **2009**, *10*, 799.
- Naseri, N.; Amiri, M.; Moshfegh A. Z. *J. Phys. D – Appl. Phys.* **2010**, *43*, 105405.
- Navalon, S.; de Miguel, M.; Martín R.; Alvaro, M.; Garcia, H. *J. Am. Chem. Soc.* **2011**, *133*, 2218.
- Kafizasa, A.; Kellicia, S.; Darra, J. A.; Parkin, I. P. *J. Photochem. & Photobiol. A-Chem.* **2009**, *204*, 183.
- Valden, M.; Lai, X.; Goodman, D. W. *Science* **1998**, *281*, 1647.
- Sakurai, H.; Tsubota, S.; Haruta, M. *Applied Catalysis A-General* **1995**, *102*, 125.
- Li, X.; Fu, J.; Steinhart, M.; Kim, D. H.; Knoll, W. *Bull. Korean Chem. Soc.* **2007**, *28*, 1015.
- Schmid, G. *Chem. Rev.* **1992**, *92*, 1709.
- Jo, K.; Kang, H. J.; Yang, H. *Bull. Korean Chem. Soc.* **2011**, *32*, 728.
- Cheow, W. S.; Li, S.; Hadinoto, K. *Chem. Eng. Res. & Design* **2010**, *88*, 673.
- Chou, J.; McFarland, E. W. *Chem. Commun.* **2004**, *14*, 1648.
- Dasog, M.; Scott, R. W. *J. Langmuir* **2007**, *12*, 3381.
- Sandhyarani, N.; Pradeep, T. *Chem. Phys. Lett.* **2001**, *338*, 33.
- Brewer, N. J.; Rawsterne, R. E.; Kothari, S.; Leggett, G. J. *J. Am. Chem. Soc.* **2001**, *123*, 4089.
- Ducker, W. A.; Senden, T. J. *Langmuir* **1992**, *8*, 1831.
- Binnig, G.; Quate, C.; Gerber, G. *Phys. Rev. Lett.* **1986**, *56*, 930.
- Derjaguin, B. V.; Landau, L. *Acta Physicochem.* **1941**, *14*, 633.
- Cleveland, J. P.; Manne, S.; Bocek, D.; Hansma, P. K. *Rev. Sci. Instrum.* **1993**, *64*, 403.
- Derjaguin, B. V. *Trans. Faraday Soc.* **1940**, *36*, 203.
- Israelachvili, J. N.; Adams, G. E. *J. Chem. Soc. Faraday Trans.* **1978**, *74*, 975.
- Shuin, V.; Kekicheff, P. *J. Colloid Interface Sci.* **1993**, *155*, 108.
- Parker, J. L.; Christenson, H. K. *J. Chem. Phys.* **1988**, *88*, 8013.
- O'Shea, S. J.; Welland, M. E.; Pethica, J. B. *Chem. Phys. Lett.* **1994**, *223*, 336.
- Derjaguin, B. V. *Kolloid Z.* **1934**, *69*, 155.
- Hartmann, U. *Phys. Rev. B* **1991**, *43*, 2404.
- Israelachvili, J. N. *Intermolecular & Surface Forces*; Academic Press: New York, 1991; pp 183-188, 275-282.

30. Feiler, A.; Jenkins, P.; Ralston, J. *Phys. Chem. Chem. Phys.* **2000**, 2, 5678.
 31. Verwey, E. J. W.; Overbeek J. T. G. *Theory of the Stability of Lyophobic Colloids*; Elsevier: New York, 1948; pp 51-63.
 32. Hogg, R.; Healy, T. W.; Fuerstenau, D. W. *Trans. Faraday Soc.* **1966**, 62, 1638.
 33. Hunter, R. J. *Foundations of Colloid Science*; Oxford University Press: Oxford, U.K., 1987; pp 397-409.
 34. Chan, D. Y. C.; Pashley, R. M.; White, L. R. *J. Colloid Interface Sci.* **1980**, 77, 283.
 35. Parker, J. L. *Surf. Sci.* **1994**, 3, 205.
 36. Park, J.-W.; Ahn, D. J. *Colloids & Surf. B: Biointerf.* **2008**, 62, 157.
 37. Ducker, W. A; Senden, T. J.; Pashley, R. M. *Nature* **1991**, 353, 239.
 38. Horn, R. G; Smith, D. T.; Haller, W. *Chem. Phys. Lett.* **1989**, 162, 404.
 39. Pashley, R. M. *J. Colloid Interface Sci.* **1981**, 83, 531.
-